(11) de Feijter, J. A.; Benjamins, J.; Veer, F. A. *Biopolymers* **1978**, *17*, 1759.
(12) de Feijter, J. A.; Benjamins, J. *J. Colloid Interface Sci.* **1981**, *81*, 91.
(13) Graham, D. E.; Phillips, M. C. *J. Colloid Interface Sci.* **1979**, *70*, 403.
(14) Sano, M.; Kawaguchi, M.; Chen, Y.-L.; Skarlupka, R. J.; Chang, T.; Zografi, G.; Yu, H. *Rev. Sci. Instrum.* **1986**, *57*, 1158.
(15) Sauer, B. B.; Yu, H.; Tien, C.-f.; Hager, D. F. *Macromolecules* **1986**, *20*, 393.
(16) Lange, H. *J. Colloid Interface Sci.* **1965**, *20*, 50.
(17) Sauer, B. B. Ph.D. Thesis, University of Wisconsin, Madison, 1987.

(18) Amis, E. J.; Janmey, P. A.; Ferry, J. D.; Yu, H. *Macromolecules* **1983**, *16*, 441.
(19) Koppel, D. J. *J. Chem. Phys.* **1972**, *57*, 4814.
(20) Kawaguchi, M.; Sauer, B. B.; Yu, H. submitted for publication in *Macromolecules*.
(21) Levich, V. G. *Physicochemical Hydrodynamics*; Prentice-Hall: Englewood Cliffs, NJ, 1962; p 603.
(22) Kramer, L. *J. Chem. Phys.* **1971**, *55*, 2097.
(23) Fowkes, F. M. *J. Phys. Chem.* **1963**, *67*, 1094.
(24) Langmuir, I.; Schaefer, V. J. *J. Am. Chem. Soc.* **1937**, *59*, 2400.
(25) Schaefer, D. W.; Han, C. C. In *Dynamic Light Scattering*; Pecora, R., Ed.; Plenum Press: New York, 1985; pp 181–243.
(26) Delahay, P.; Trachtenberg, I. *J. Am. Chem. Soc.* **1957**, *79*, 2355.

# Holography as a Tool for Mechanistic and Kinetic Studies of Photopolymerization Reactions: A Theoretical and Experimental Approach

**C. Carre,\* D. J. Lougnot, and J. P. Fouassier**

*Laboratoire de Photochimie Générale, Unité Associée au CNRS No. 431, Ecole Nationale Supérieure de Chimie, 3 rue A. Werner, 68093 Mulhouse Cedex, France.*

ABSTRACT: An original method based on the study of the time evolution of the refractive index modulation that results from a spatially inhomogeneous polymerization is developed with an aim at providing information on the initiation mechanism of the reaction. This study is restricted to the case where the intensity response of the material is not linear, i.e., when the polymerization rate is proportional to the square root of the absorbed dose of light. The equations that are arrived at are deduced from the simultaneous study of the bleaching of the sensitizer, the conversion of the monomer, and the diffusion of the species involved. The interest of this original approach for the study of the reactivity of polymerizable mixtures is exemplified by a concrete application. The system used to demonstrate the promising character and the flexibility of this nondestructive technique utilizes the photoredox reaction of methylene blue in its triplet state with an electron donor, as the source of initiating species. By use of the time-resolved holographic technique, the yield of the initiation step of this polymerization, which is almost impossible to measure by classical techniques, can be readily determined in the highly viscous environment of an incipient polymer film. Moreover, several pieces of mechanistic information can be collected from the kinetic study of the hologram growth curves.

## 1. Introduction

During recent years, holographic techniques have drawn the attention of many physical chemists owing to their potent applications as a nondestructive means for the study of physical transformations that occur in particular media where the conventional methods of investigation cannot be put into operation. One of the most immediate applications of these techniques is the study of local deformations or microdisplacements.[1,2] They have also been used for the production of holographic optical elements such as gratings, lenses, or prisms with better performances than conventional optical components or for the design of optical memories, able to store large amounts of information in small volumes of photosensitive materials.

The kinetic analysis of chemical reactions conducted in photopolymerizable films is another very interesting field in which holographic techniques show promise.[3-6] Thus, highly viscous or solid systems form an attractive class of compounds that lend themselves to this type of investigation.[7-10]

In fact, in such systems, polymerization takes place only in the bright areas of the pattern created by the interference of two plane waves, and volume-phase holograms exhibiting high diffraction efficiencies are created. However, a better comprehension of the physical and chemical processes that induce the refractive index modulation in a photopolymerizable active material is still required.

In this context, great care must be taken when dealing with the available theories that are generally used to rationalize the experimental observations and draw information from the study of the building up of the hologram.

The propagation of optical waves in thick gratings has been studied thoroughly, and it is possible in the present state of the art, to calculate from the theoretical analysis, the amplitude, phase, or polarization of the waves emerging in the reconstruction step.[10,11] Owing to the periodicity of the interference pattern, a Fourier representation of the grating can be employed. With this approach, the general coupled wave theory allows the first and higher orders diffraction efficiencies to be examined for a given grating with any index profile. The approach introduced by Kogelnik for thick sinusoidal gratings that uses simple analytical expressions leads to satisfactory analysis provided the underlying assumptions are satisfied.[12]

Braüchle and Burland have exemplified the usefulness of holography in many systems where the spatial modulation of the refractive index or of the absorption coefficient has the same profile as the interference pattern.[3] In particular, they used this technique with continuous-wave lasers to obtain detailed information on reversible or irreversible photoprocesses (rate constants, quantum yields, number of photons involved in a process, polymer lengths, etc.). For this type of applications, they are satisfied with using the Kogelnik expression reduced to its first two
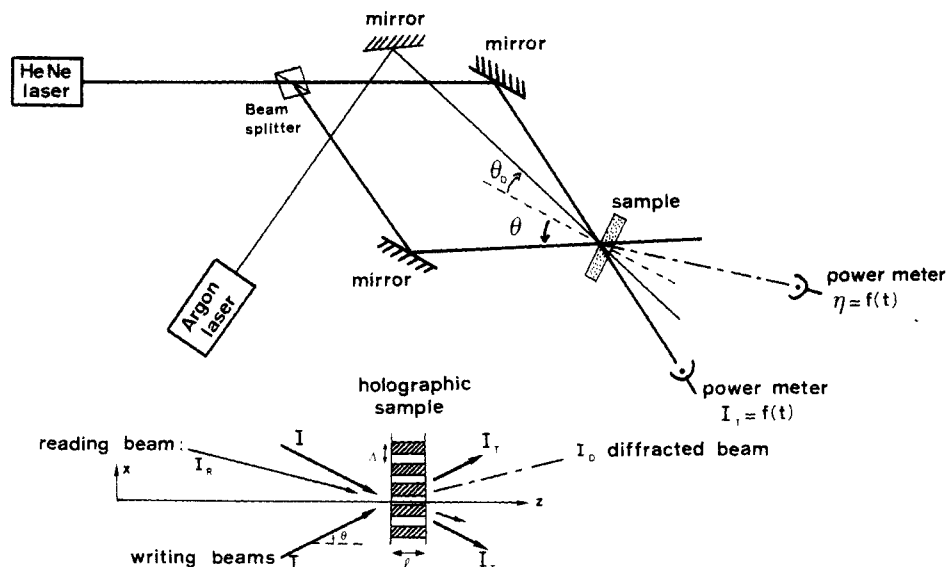
**Figure 1.** Experimental setup used to record the growth of the holographic curves.

terms. Thus, the growth of the holographic curves related to a simple one-step reaction is a quadratic function of the irradiation time for the early moments of the recording process. After this initial period, the refractive index profile has to be described by a Fourier expansion.

When the holographic recording results from the superposition of several photoprocesses, changing the wavelength of the probe beam or the fringe spacing can help separate the various contributions. Doing so, Pinsl et al. were able to monitor separately and simultaneously amplitude and phase gratings in solid matrixes by using phase-modulated holography.[3] Thus, interesting conclusions can be drawn on photoinduced matrix effects, and direct measurement of photochemical quantum yields is possible.

In the case of photopolymerizable recording systems, the interference pattern is due to the spatially inhomogeneous polymerization of a monomer. Under usual conditions of irradiation, i.e., when the reaction rates are proportional to the square root of the absorbed dose,[13] the index modulation cannot be assumed to exhibit a sinusoidal profile, and the expression for the diffraction efficiency of mixed gratings in the case of unslanted gratings and Bragg incidence introduced by Kogelnik cannot be resorted to. In this work, an alternative treatment is introduced that should be easily accessible to chemists and that could allow some typical kinetic parameters to be estimated in the case of photopolymerization reactions conducted in films. Our purpose is not to try to predict from some theoretical analysis the diffraction efficiency of an hologram at a given time but rather to turn the curve $\eta = f(t)$ to account to draw information on the kinetics of the initiation step of a photopolymerization and to elucidate mechanistic points in the overall initiation scheme.

## 2. Experimental Details

**2.1. Holographic Setup.** The experimental setup is shown in Figure 1. The hologram is created with a HeNe laser ($\lambda$ = 633 nm). The writing light is split into two beams of equal intensity. A system of adjustable mirrors allows the beams to interfere with equal path lengths at a full angle $2\theta$ of about 25°. With such a geometric arrangement, the fringe spacing ($\Lambda$) is 1.42 $\mu$m.

The HeNe laser beam is expanded and its size is limited by a diaphragm so that the incident power density at the sample is 47 mW/cm² for a spot size of 0.3 cm. In that case, the interference pattern can be considered to be due to the superposition of two coherent plane waves.

The hologram is read with an argon ion laser (Spectra Physics Model 171). The diameter of the reading beam is reduced to a size narrower than that of the interference pattern (0.1 cm) by proper focusing; its power density is then 18 mW/cm² at 488 nm. The intensity of the diffracted light is measured by a power meter (Chauvin et Arnould) connected to a chart recorder, and the diffraction efficiency is defined as the ratio of the intensity of the diffracted beam $I_D$ to that of the reading beam $I_R$. The interest in measuring the hologram efficiency at 488 nm lies in the fact that the reading beam is almost inactive toward the recording material at this wavelength. Thus it becomes possible to record the building up of the hologram as a function of the irradiation time without perturbing the refractive index modulation. The Bragg condition has to be fulfilled ($\theta_D$ = 10°) to achieve maximum efficiencies.

With a second detector in the path of the red beam, it is also possible to record the transmittance of the sample, i.e., the average concentration of the sensitizer, as a function of the irradiation time.

**2.2. Sample Preparation.** The polymerizable systems used in the experiments reported here were developed following the basic ideas suggested by Sugawara et al.[14] The sample contains a solventless mixture of mono- and difunctional acrylamides,[38] dimethylacrylamide (DMAA) as the solvent (650 g/L), acrylamide (AA) as the thickening agent (410 g/L), and methylenebis-(acrylamide) (MBAA) as the cross-linker (70 g/L); a preexposure at 313 nm is required to increase the viscosity of the system so as to allow spreading onto glass plates. This prepolymerization is conducted with a medium-pressure mercury arc (Philipps HPK 125 W) during 20 min at an irradiation power density of 3 mW/cm². AA and MBAA were purified by multiple crystallization in ether/methanol mixtures. DMAA was used as received, without further purification. The sensitizer was methylene blue (MB), which exhibits high absorption at 633 nm and which is almost transparent at 488 nm. Five amines—primary to tertiary—will be considered in this study (Table I) (the amines studied in this work were of the highest available grade from Aldrich Chemical).
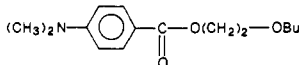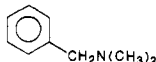
The samples were prepared by embedding the sensitive mixture between two glass plates separated by an appropriate Mylar film spacer so as to obtain a constant thickness ($l$ = 80 $\mu$m, [MB] = 3 × 10⁻³ M and [amine] = 0.8 M).

The UV and IR absorption spectra were recorded on a Beckman DU 7 and a Perkin-Elmer 781 spectrophotometers. For IR measurements the samples were prepared between NaCl plates, and their thickness was 50 $\mu$m. The intensities of the IR absorptions were determined at 20 °C by measuring the characteristic bands of AA at 810 cm⁻¹ and of DMAA at 790 cm⁻¹.

## 3. Hologram Building Up

**3.1. Mechanism.** The hologram is photochemically induced by the writing beams in the regions of constructive

<div align="center">

**Table I**

**Holographic Results for the System MB + Acrylamides + Amine$^a$**

</div>

| amine | | | $\eta_{max}$, % | $(K\phi_{MB})_{TEA}$ | $(\phi^{1/2}/K\phi_{MB})_{TEA}$ | $(\phi)_{TEA}$ | $10^{-9}K_{CT}$,$^b$ M$^{-1}$ s$^{-1}$ |
|---|---|---|---|---|---|---|---|
| triethanolamine | N(CH$_2$CH$_2$OH)$_3$ | TEA | 2.0 | 1 | 1 | 1 | |
| diethanolamine | HN(CH$_2$CH$_2$OH)$_2$ | DEA | 1.8 | 1.5 | 0.48 | 0.52 | |
| ethanolamine | H$_2$NCH$_2$CH$_2$OH | EA | 1.6 | 1.9 | 0.5 | 0.94 | 1.7 |
| 2-butoxyethyl 4-(dimethylamino)benzoate | (CH$_3$)$_2$N—⟨O⟩—C—O(CH$_2$)$_2$—OBu ‖ O | BEA | 10 | 0.5 | 0.17 | 8 × 10$^{-3}$ | 9.8 |
| dimethylbenzylamine | ⟨O⟩ CH$_2$N(CH$_3$)$_2$ | DMBA | 0 | 2.9 | 0 | 0 | 1.4 |

$^a$ $(x)_{TEA}$: relative value of $x$ with TEA for reference. $^b$ $K_{CT}$: this constant is determined in DMAA as the solvent.

interference corresponding to the bright fringes. The photoinitiator absorbs light in these regions and is converted to its triplet state by intersystem crossing. Then, a redox reaction takes place between the dye molecule and the amine that generates free radicals capable of initiating the polymerization of the monomer mixture. If this process is fast, the diffusion of the active species is limited and only the areas of highest intensity undergo photopolymerization.

It is also important to observe that diffraction becomes effective only after a more or less important induction period of time which is related to the inhibiting effect of impurities and oxygen dissolved in the system. In fact, the photopolymerization, which is a radical initiated chain reaction, cannot start up before all the inhibitor is consumed.

The result of this polymerization is a spatial modulation of the refractive index that images the incident intensity pattern:

$$I(x) = 2I\left\{1 + \cos\left(\frac{2\pi}{\Lambda}x\right)\right\} \qquad (1)$$

where $\Lambda$ represents the fringe spacing and $I$ the intensity of the two incident beams.

As the reaction proceeds, the concentration of available monomer molecules decreases slowly and concomitantly a very efficient bleaching of the sensitizer takes place in the areas where the intensity is the highest. The resulting gradient of concentration causes additional MB to diffuse from the dark regions. For that reason, the optical density modulation is a complicated function of the spatial coordinate $x$. Since, under our experimental conditions, less than 15% of the monomer disappears and the diffraction efficiencies do not exceed 5%, the diffusion of the monomer will not be taken into account.

Under the experimental conditions prevailing, the refractive index changes can be considered essentially caused by the polymerization reaction.[9]

Two approximations have been introduced to establish a mathematical relation between the gratings formation, the dye's bleaching, and the polymerization.

The rate of the photochemically induced polymerization ($R_p$) is assumed to remain proportional to the square root of the absorbed dose as it is in solution.[13] By measurement of the intensity of the IR absorption at 790 cm$^{-1}$ before and after irradiation for a given period of time with one of the red beams, the percent of double bonds having disappeared ($\rho$) can be determined as a function of the incident intensity ($I$; see Appendix): the curve $\rho = f(I^{1/2})$ is a straight line in acrylamides films (Figure 2). This assumption remains valid as long as the incident light intensity is low; with higher intensities, rates of polymerization increasing linearly with $I_{abs}$ were reported by several authors.[15]
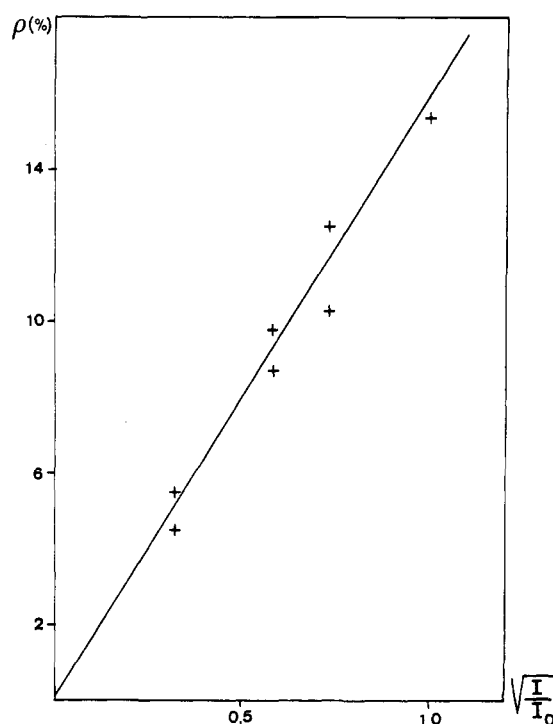


**Figure 2.** Percent of double bonds having disappeared as a function of the square root of the incident intensity under homogeneous irradiation.

Thus under holographic conditions (spatially modulated irradiation), $R_p$ can be represented by the following expression:

$$R_p(x,t) = k[\bar{M}](\phi I_{abs}(x,t)/l)^{1/2} \qquad (2)$$

where $k$ is a constant that characterizes the matrix, $[\bar{M}]$ the average monomer concentration, and $\phi$ the overall initiation yield of the photopolymerization (i.e., the number of starting chain per photon absorbed). $I_{abs}(x,t)$ represents the spatiotemporal distribution of the absorbed dose:

$$I_{abs}(x,t) = 2I\left\{1 + \cos\left(\frac{2\pi}{\Lambda}x\right)\right\}(1 - 10^{-OD(x,t)}) \qquad (3)$$

with $OD(x,t)$ standing for the optical density at time $t$ at the point of abscissa $x$. The local percent of double bonds having disappeared ($\rho$) is finally given by

$$\rho(x,t) = (100/[\bar{M}])\int_{t_0}^{t} R_p \, dt + \rho(t_0)$$

$$\rho(x,t) = 100k\left(\frac{2I\phi}{l}\right)^{1/2}\left(1 + \cos\left(\frac{2\pi}{\Lambda}x\right)\right)^{1/2}A(x,t) + \rho(t_0) \qquad (4)$$

$$A(x,t) = \int_{t_0}^{t}(1 - 10^{-OD(x,t)})^{1/2} \, dt$$

where $t_0$ represents the induction period.

On the other hand, this treatment assumes that the empirical correlation between the refractive index of a solution containing polymer such as styrene or methyl methacrylate and its concentration[16] holds under our conditions. The refractive index ($n$) increases linearly with the decrease of double bonds as the polymerization proceeds. With this approach, the mathematical expression of $n$ as a function of the irradiation time ($t$) and of the spatial coordinate ($x$) is the following:

$$n(x,t) = n_0 + 2^{1/2}NA(x,t)(1 + \cos 2\pi x/\Lambda)^{1/2} \quad (5)$$

$$= n_0 + 2^{1/2}NA(x,t)|\cos \pi x/\Lambda|$$

where $N$ is a constant depending on the polymerizable system and $n_0$ the refractive index of the initial mixture.

Since $OD(x,t)$ is a spatially periodic function, $A(x,t)$ exhibits the same spatial characteristics and is also a periodic function. As a consequence $n$ remains a periodic function of $x$ with the same period (fringe separation) as $I(x)$, but it is not a sinusoidal function. Therefore, the response of the recording material under the experimental conditions prevailing is not linear. Even though, strictly speaking, the theoretical approach developed by Burland and Bräuchle[3] could be adapted to the $I^{1/2}$ case, indeed, the mathematical expressions become more complex in this instance and difficult to handle.

Shibata and Johnson have introduced an analytic expression accounting for the diffraction efficiency in the case of nonsinusoidal absorption gratings created by a square-wave profile.[17] Tomlinson[18] and Urbach and Meier[19] have considered the effect of attenuating the exciting beams in relation with the saturation of the actinic transition in the sample. The time dependence of the diffraction efficiency is very complicated, and this approach can be used only in particular situations where simplifications can be justified. Richter et al.[20] have reported that the diffraction intensities in the higher orders exceeded by far the values expected from the theory and a nonsinusoidal profile of the hologram was assumed in order to explain this observation. They introduced a function $f(x)$ accounting for the shape of the grating that is progressively defined by trial and error from the analysis of the diffraction intensities in the higher orders, and they got an excellent agreement between the measured and calculated values. However, in this physical approach, no interpretation taking into account the solid-state photopolymerization is proposed for the mathematical $f(x)$ expression. Magnusson and Gaylord[11] have presented a general formalism that describes the multiwave diffraction properties of thick gratings. Because of the periodicity of the grating, a Fourier series representation is employed with a coupled-mode theory of diffraction. Thus, the diffraction efficiency of a grating with any given shape can be readily calculated by using only elementary numerical techniques.

Several experimental studies devoted to gratings created by photopolymerization reactions were reported,[3,21,22] but they deal only with systems in which the response is linear, i.e., when the intensity of the writing beams is high enough to cause the polymerization rate to be proportional to the absorbed dose. In this particular case, the building up of the grating can be clearly described by the simplest expansion—to the first two terms—of the Kogelnik's relationship.

On the contrary, the experiments that are dealt with in this paper refer to polymerizations conducted in such a way that the reaction rates are proportional to the square
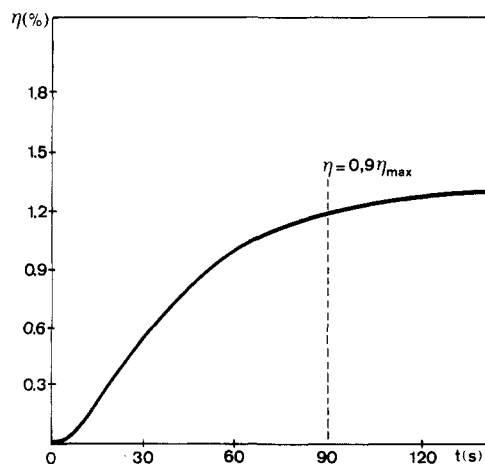


**Figure 3.** Diffraction efficiency ($\eta$) as a function of time for [MB] = $3 \times 10^{-3}$ M.

root of the absorbed dose. These conditions of irradiation are those prevailing in photopolymerization experiments when the absorbed dose is weak enough to ensure a homogeneous distribution of the initiating species and a bimolecular termination of the growing polymer chains.

Unfortunately, no analysis is available so far in the literature for the determination of kinetic parameters when the modulation of the refractive index is a complicated function of spatial coordinate $x$ because the equations that contain position and time variables cannot be solved analytically. Our approach involves the study in parallel of the building up of the grating under holographic irradiation and of the bleaching of the sensitizer under continuous homogeneous illumination. By taking into account these results and those of the IR followup of the photopolymerization, it is possible to deduce a relationship between the diffraction efficiency and the refractive index. Thus several characteristic parameters such as the efficiency of the initiating species involved in a polymerization reaction conducted in film become readily available.

The case that corresponds to a photoinitiation process by the system MB/amine will be given special attention in the next sections.

**3.2. Photopolymerization in the Presence of MB Alone.** When no amine is present in the medium, the diffraction efficiencies do not exceed 1%. Though the general shape of the $\eta(t)$ curves (Figure 3) looks like normal $t^2$ hologram growth, a careful examination of their first part shows a dependence of $\eta$ that is not really quadratic with the irradiation time. The polymerization actually starts up after a certain time of illumination, and the duration of this period is related to the amount of oxygen dissolved in the medium. After this "induction period", $\eta$ increases with the exposure, then saturates, and reaches a plateau.

The poor efficiencies achieved in these systems are due to the fact that $^3$MB undergoes a self-quenching process generating the demethylated forms of MB (these demethylated MBs are called azures). This reaction competes with the photooxidation–reduction by acrylamide monomers which yields the initiating radical species.[24-26]

Owing to the complexity of the general reaction scheme and to the fact that the photoproducts (azures) are also active, any kinetic analysis of the bleaching of the sensitizer is impossible.

**3.3. Photoinitiation by the System MB/Amine. 3.3.1. Study of the Transmitted Light Intensity at 633 nm.** In this case, the photoredox system consists of methylene blue as the oxidant and amine as the reductant.[14,27] As a rule, in these systems, MB disappears faster
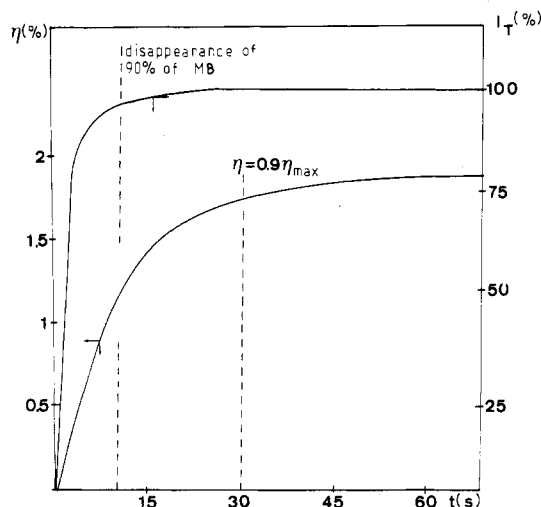
**Figure 4.** Transmitted intensity ($I_T$) of each writing beam under holographic exposure at 633 nm and diffraction efficiency ($\eta$) as a function of time for [MB] = 5 × $10^{-3}$ M in the presence of DEA ([DEA] = 1 M).

from the medium than in the absence of electron donor except when BEA is present. The curves $\eta = f(t)$ and $I_T = g(t)$ (Figure 4) can be divided into three parts. In this paper, only the part of the curve corresponding to a rapid increase of the diffraction efficiency to 75% of its maximum will be dealt with. This part corresponds to the stage of the polymerization during which a linear correlation between the diffraction efficiency and the degree of conversion measured by IR is experimentally observed (see section 3.3.3).

**3.3.1.1. First Part of the Holograms.** In spite of the fact that 75% of the dye is consumed during the very first moments—4–5 s—the diffraction efficiency does not exceed 0.5%.

On the basis of a preliminary study by time-resolved laser spectroscopy, the findings of which are reported elsewhere,[24] the hologram growth can be interpreted as follows: at the beginning of the holographic experiment, the concentration of the sensitizer is high (>$10^{-3}$ M) and the main decay pathway of $^3$MB involves the reaction with another MB molecule to form demethylated MBs (azures) as in the absence of amine. No polymerization takes place until all the inhibitors have reacted since their affinity for free radicals is much greater than that of the monomer.

Though the growth of the hologram looks again in its early stage like a $t^2$ dependence,[3] it seems unreasonable to try to fit it by invoking the Kogelnik theory at the risk of overinterpreting the experimental results. On that account, we have restricted the investigation of the polymerization reaction to the second part of the hologram growth in which this problem can be disregarded.

**3.3.1.2. Second Part of the Holograms.** In the second part of the experiment (4 s < $t$ < 8 s), $\eta$ increases rapidly and reaches 75% of its maximum value obtained at infinite exposure. The transmission of the sample at 633 nm increases to about 95%.

The sensitizer concentration gradient in the sample rises as the result of its inhomogeneous bleaching. The variation of MB concentration in the brightest areas is caused by two processes working in opposite directions: the chemical bleaching of the dye (negative contribution) and the diffusion from the dark areas (positive contribution).[6] The complete temporal and spatial description of the kinetic behavior of this system for a given value of the spatial coordinate $x$ can be expressed as follows:

$$-\frac{1}{\epsilon l}\frac{d}{dt}\{OD(x,t)\} = \frac{\phi_{MB}}{l}\{I_{abs}(x,t)\}^{\alpha} - D_{MB}\nabla^2\{OD(x,t)\} \quad (6)$$

where $D_{MB}$ stands for the diffusion coefficient of MB according to Fick's law, $\phi_{MB}$ is the overall quantum yield for the bleaching of MB, $\alpha$ is the photochemical order of the reaction in the film, $\epsilon$ is the molecular extinction coefficient at 633 nm, and $l$ is the sample thickness. Since this equation does not accept any analytic solution, several approximations are introduced to simplify the description of the experimental results.

The mathematical treatment used here has been suggested by the following experiment. The sample is irradiated alternately under holographic and homogeneous conditions, and the transmitted intensity of the permanent beam is recorded.

Under this particular type of illumination, $I_T$ is observed to increase continuously irrespective of the changes introduced by turning the second laser beam off. This observation is a sign that no gradient of concentration can be detected with the time responses and switching frequencies used in this work (typically 0.1 s). As a consequence the diffusion of the sensitizer is faster than its bleaching, and this second process governs the kinetics of the overall process, at least for photopolymerizable systems with low viscosity.

Under stationary holographic conditions, the diffusion term of eq 6 is then assumed to be proportional to the chemical term; i.e., the flow of molecules diffusing to the illuminated (and bleached) areas is proportional to the bleaching rate:

$$-\frac{d}{dt}(OD(x,t)) = K\phi_{MB}(I_{abs}(x,t))^{\alpha} \quad (7)$$

$K$ is a constant that depends on the chemistry of the system and on the irradiation setup.

By analogy with the formalism used for the kinetic treatment of photobleaching as a function of the absorbed dose,[23] the microscopic parameters $I_{abs}(x,t)$ and $OD(x,t)$, which account for the behavior of the species at the scale of the fringe spacing ($\Lambda \sim 1$ $\mu$m), are replaced by macroscopic parameters: the intensity absorbed by the sample ($2I_{abs}$) and the macroscopic optical density under holographic exposure (OD).

The equation that describes the kinetic behavior of the system reduces then to

$$-\frac{d}{dt}(OD) = K\phi_{MB}(2I_{abs})^{\alpha} = K\phi_{MB}(2I)^{\alpha}(1 - 10^{-OD})^{\alpha} \quad (8)$$

and after integration

$$B_{\alpha}(t) = \int_{OD_{t=0}}^{OD_t} \frac{d(OD)}{(1 - 10^{-OD})^n} = K\phi_{MB}(2I)^{\alpha}t \quad (9)$$
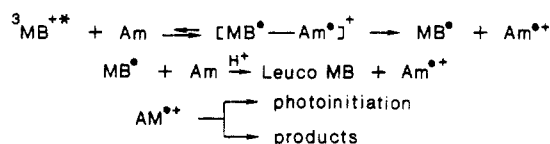
The correctness of this mathematical treatment is corroborated by the following observation: regardless of whether the irradiation is conducted under holographic or homogeneous conditions, the plot of the parameter $B_{\alpha}(t)$—which is related to the sensitizer concentration recorded as a function of time by the 633-nm laser—versus time (Figure 5) is linear for $\alpha = 1$. Moreover, the slope of this straight line is also observed to increase linearly with the incident intensity, hence the conclusion that the photoreaction is first order and that this type of treatment in which macroscopic parameters are substituted for microscopic ones is self-consistent.

In this part of the curve, the major decay pathway of $^3$MB is the reaction with the amine synergist to form MB$^{\bullet}$ and an amine-derived radical that can initiate the polym-
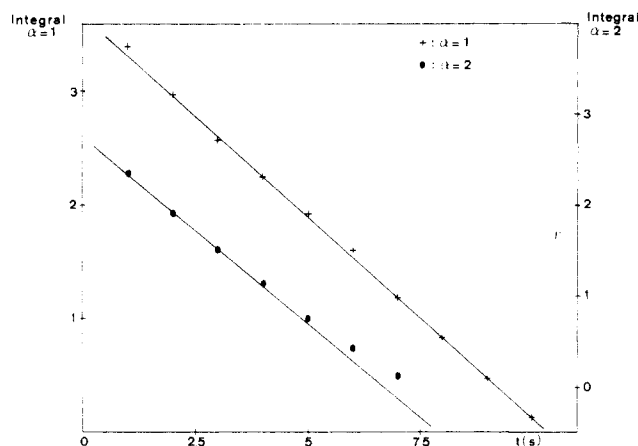
**Figure 5.** Integral $(\int_{OD_0}^{OD_t} dOD/(1 - 10^{-OD})^\alpha)$ as a function of time for the determination of the photochemical order ($n$) of the MB bleaching in the presence of an amine (DEA).



**Figure 6.** Diffraction efficiency ($\eta(t)$) as a function of the spatial average percent of polymerized monomers ($\bar{p}(t)$) in the case of DEA.

erization.[14,28] The radicals mainly disappear by reacting with a second amine molecule. This reactional scheme

$$^3\text{MB}^{+*} + \text{Am} \rightleftharpoons [\text{MB}^\bullet\!-\!\text{Am}^\bullet]^+ \rightarrow \text{MB}^\bullet + \text{Am}^{\bullet+}$$

$$\text{MB}^\bullet + \text{Am} \xrightarrow{H^+} \text{Leuco MB} + \text{Am}^{\bullet+}$$

$$\text{AM}^{\bullet+} \begin{cases} \rightarrow \text{photoinitiation} \\ \rightarrow \text{products} \end{cases}$$

agrees with $\alpha = 1$. The comparison of the slopes of the lines $B(t) = f(t)$ allows thus the efficiency of the photoreduction of MB by the different amines under study to be estimated. These results are reported in Table I.

**3.3.1.3. Third Part of the Holograms.** In the last part of the curves, most of the dye molecules are irreversibly photobleached and $\eta$ reaches a plateau. In effect, the factor that limits the growth of the diffraction efficiency is the bleaching of the sensitizer.

**3.3.1.4. The Particular Case of BEA.** The case of BEA is somewhat different: the bleaching of the dye is not so fast, and more MB molecules are present in the sample during the growth of the hologram. From the very beginning of the writing process, the photochemical order of the bleaching reaction remains 1, which indicates a very efficient interaction of MB with BEA as compared with what is observed with ethanolamines.

**3.3.2. Results.** During the growth of the hologram (4 s $< t <$ 8 s), the concentration of the sensitizer is no longer important. We assume that the index modulation is induced by the polymerization of the acrylamide mixture.[8] Léger et al. and Coutandin et al.[29] have investigated successfully the self-diffusion of polystyrene chains labeled with fluorescein by using holographic techniques. Recently, Smith[30] showed how "fluorescence redistribution after pattern photobleaching" can be used to study the diffusion of polymer molecules in the melt: as fluorescent molecules diffuse from the dark regions of the sample to the illuminated regions, the total observed fluorescence intensity increases. Zhang and Wang[31] have introduced host dye molecules in a polymer network and investigated the influence of polystyrene cross-linking on the diffusion coefficient of camphorquinone. These different works and results of Woppschall et al.[32] led us to consider that the monomer diffusion can be disregarded in the second part of the curve as long as the conversion does not exceed 15%. Thus, the refractive index would not be very different from that of the starting material in the dark areas of the gratings.

After having increased monotonically, $\eta$ reaches a plateau that is mostly due to the irreversible bleaching of the
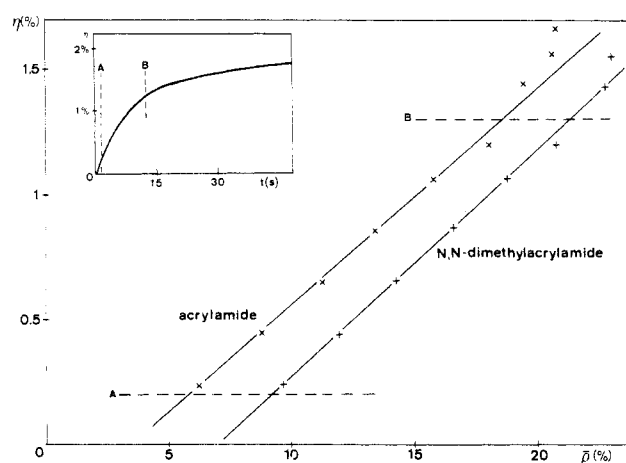
sensitizer. The results in Table I show that the best holographic efficiency is achieved in the presence of BEA. In this case, MB is bleached slowly so that the diffraction efficiency grows during more than 10 min and the writing process can proceed to a higher result than with ethanolamines. After the first minute, the diffusion of the monomer to the brightest areas has to be taken into consideration, and the mathematical treatment that has been introduced to account for the second part of the hologram is not valid with this compound.

On the other hand, no hologram is created in the presence of DMBA, though the reaction between this amine and the triplet state of the sensitizer is very efficient. It is inferred from this observation that the radical species arising from the oxidation–reduction is not able to react with monomer molecules and to initiate a polymerization.

**3.3.3. Second Part of the Hologram Growth: Correlations with IR Measurements.** For correlation of the hologram growth with the monomer conversion, the concentration of double bonds is determined by IR spectroscopy as a function of the irradiation time ($t$) under holographic exposure. The spatial average percent of polymerized monomers ($\bar{p}(t)$) is deduced from the transmission measured at 790 or 810 cm$^{-1}$ before and after irradiation. With the four amines considered, the curve $\eta(t)$ as a function of $\bar{p}(t)$ is clearly a straight line in the second part of the hologram growth. In the case of DEA, the following relationship is deduced (Figure 6) from the experimental results:

$$\eta(t) = a\bar{p}(t) - b \tag{10}$$

$a$ and $b$ are two parameters that depend on the polymerizable matrix and on the irradiation device.

In the first part, $\eta(t)$ remained almost zero. Since at time, $t_0$, i.e., when $\eta$ begins to grow, the following expression holds true:

$$\eta(t_0) = 0 = a\bar{p}(t_0) - b$$

We can write for the second part

$$\eta(t) = a(\bar{p}(t) - \bar{p}(t_0))$$

in which $\eta$ appears to be proportional to $[\bar{p}(t) - \bar{p}(t_0)]$.

Since the conversion does not exceed 15%, the refractive index is assumed (vide supra) to linearly increase with this percent of conversion. The refractive index modulation $n_1(t)$ is then the difference between the indexes of the polymerized ($n$) and unpolymerized areas ($n_0$):

$$n_1(t) = n - n_0 \propto \bar{p}(t) - \bar{p}(t_0)$$

As $n_1(t)$ is proportional to $\bar{p}(t) - \bar{p}(t_0)$, it is deduced from (10) that

$$\eta \propto n_1$$

In the coupled-wave theory for thick holographic gratings,[12] the diffraction efficiency of a phase hologram is approximated by

$$\eta = \left(\frac{\pi n_1 d}{\lambda \cos \theta}\right)^2 \quad (11)$$

which shows that $\eta$ is proportional to the square of the index modulation $n_1$.

In the classical systems that obey the Kogelnick theory[3] as well as in those developed in this work, the irradiation pattern is a sinusoidal function but the responses are basically different; the rate of a radical polymerization is proportional to the square root of the absorbed dose, and therefore the response of the system cannot be linear.

**3.3.4. Mathematic Study of the $\eta(t)$ Curves.** With the same approach as the one introduced in section 3.3.1.2 (OD is defined by (8) instead of (6) in (4)), the average percent of double bonds polymerized $\bar{p}(t)$ can be expressed by

$$\bar{p}(t) = 100k(2I\phi/l)^{1/2} \int_{t_0}^{t} (1 - 10^{-OD})^{1/2}\, dt + \bar{p}(t_0)$$

In the case of a first-order photoreaction, this can be rewritten as follows:

$$\bar{p}(t) = -100\frac{k\phi^{1/2}}{K\phi_{MB}(2Il)^{1/2}} \int_{OD_{t_0}}^{OD_t} \frac{dOD}{(1 - 10^{-OD})^{1/2}} + \bar{p}(t_0)$$

$$(12)$$

with

$$dOD/dt = -2IK\phi_{MB}(1 - 10^{-OD}) \quad (8)$$

When combined with (10), it is finally deduced that

$$\eta(t) = -100\frac{ak\phi^{1/2}}{K\phi_{MB}(2Il)^{1/2}}B_{1/2}(t) + \text{constant} \quad (13)$$

with

$$B_{1/2}(t) = \int_{OD_{t=0}}^{OD_t} dOD/(1 - 10^{-OD})^{1/2}$$

As expected, straight lines are arrived at when displaying the diffraction efficiencies obtained with the different amines as functions of $B_{1/2}(t)$ (Figure 7). This observation must be regarded as corroborative evidence in favor of the approximations and assumptions that were introduced in the development of this treatment. As the parameters $a$ and $k$ are related to the chemistry of the mixture and to the experimental setup, the slopes of the straight lines allow the ratio $\phi^{1/2}/K\phi_{MB}$ to be estimated in relation to the others. These relative values are reported in Table I, in which TEA is taken as a reference.

## 4. Discussion

**4.1. Reaction Scheme.** The transient intermediates ($^3MB$, $MB^{\bullet}$, etc.) which are detected in water, acetonitrile, or methanol have been studied thoroughly by many authors.[24-26,33] The $pK_a$ of these species and the electron-transfer rate constants from $^3MB$ have been determined in aqueous media.[34] Kayser and Young[28] have investigated the reduction of $^3MB$ by both alkyl- and arylamines in methanol and the decay of the corresponding semireduced species by flash techniques. They pointed out the formation of a partial charge-transfer intermediate and in-
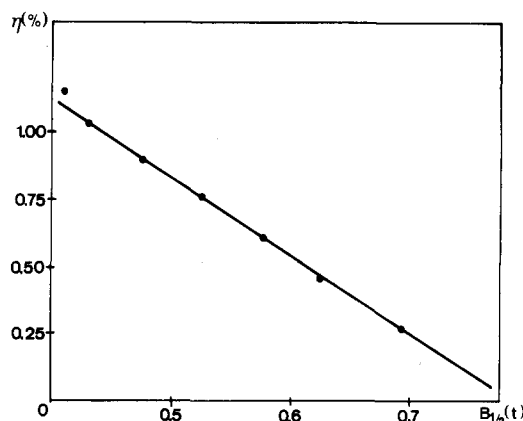


**Figure 7.** Diffraction efficiency ($\eta(t)$) as a function of the integral $B_{1/2}(t)$.

troduced mechanisms accounting for their experimental results.

The mechanism of the photopolymerization induced by the MB/amine system involves at least a dozen elementary steps. Of them, three are particularly important in the holographic recording process: the step generating $^3MB^*$ with a quantum yield $\phi_{ST}$, the step corresponding to the production of the initiating species $AM^{\bullet+}$ through reduction of $^3MB^*$ with a quantum yield $\phi_R$, and the step leading to photoinitiation of a new polymer chain with an actual yield $\phi_i$. The overall initiation yield of the polymerization used to memorize the interference pattern $\phi$ can be expressed as

$$\phi = \phi_{ST}\phi_R\phi_i$$

and the overall bleaching yield of MB as

$$\phi_{MB} = \frac{1}{2}\phi_{ST}\phi_R$$

As a preliminary, several rate constants corresponding to elementary process involved in the bleaching mechanism of MB were determined by time-resolved laser spectroscopy in aerated prepolymerized mixtures: the spontaneous decay rate of $^3MB$ to ground state ($k_D \sim 1.9 \times 10^4$ s$^{-1}$), the rate constant of the photoreduction by the prepolymerized mixture ($k_{AA} \sim 4 \times 10^3$ s$^{-1}$), and the rate of the quenching by ground-state oxygen ($k_{O_2}[O_2] = 8.5 \times 10^5$ s$^{-1}$).

In the sensitive systems containing no amine, the profile of the hologram growth curves is in good agreement with what is observed by laser spectroscopy: the holographic efficiency increases slowly and levels off rapidly, while the major decay pathway of $^3MB$ is through deactivation by oxygen.

**4.2. Comparison of the Different Amines.** The photoreduction of MB by a given amine results in a permanent bleaching of this dye and in every case determines the kinetics of the overall system.

In the presence of an amine, $^3MB$ decays through a charge-transfer complex[28] that undergoes either a complete electron transfer to a radical pair or a back electron transfer to the starting materials in their ground state. The rate constants ($k_{CT}$) that have been determined for several systems in DMAA and that are reported in Table I corroborate that, even in prepolymerized mixtures, the electron-transfer process prevails over the other deactivation pathways.

The results reported in Table I show that the highest hologram efficiencies are achieved with the system containing BEA. This superiority of the mixtures containing BEA can be readily understood from the kinetic information obtained by laser spectroscopy: the slow bleaching of MB allows the polymerization—and by way of conse-

quence, the building of the grating—to progress to maximum conversion. With alcohol amines, the bleaching mechanism remains basically the same,[35] but the electron-donating character of the nitrogen center indirectly controls the efficiency of the chanel producing the active species Am$^{\cdot+}$ and, thus, the extent of the polymerization reaction.[36,37]

The behavior of DMBA is somewhat different. With this compound, the bleaching of MB is fast, but the amine-derived radical is hopelessly unreactive toward acrylamides, hence the lack of initiation shown by $\phi$.

The important kinetic data that can be drawn from holographic measurements—to the exclusion of any other spectroscopy technique—are the relative efficiencies ($\phi_i$) of the elementary process corresponding to the creation of a new polymer chain through the action of an initiating radical on a monomer molecule. These data, collected in Table I ($\phi$), were calculated as the product of $K\phi_{MB}$ (available from laser spectroscopy experiments) by $\phi^{1/2}/K\phi_{MB}$ (obtained as the slope of the $\eta = f(B_{1/2})$ curves). It becomes, thus, possible to appreciate the relative part played by the two consecutive steps of the overall initiation mechanism: the reaction of the active species and the effective starting up of a new polymer chain.

## 5. Conclusion

This paper is concerned with the use of holographic techniques for the kinetic study of some kinds of photoinduced polymerizations. Its first part is devoted to the theoretical analysis of the bleaching of the initiator and the development of the diffraction efficiency. This approach is conspicuous by the fact that the treatment of the spatiotemporal evolution of the holographic sample that is introduced considers those processes as being interdependent. Based on the observation that, under the experimental conditions prevailing, the extent of the photopolymerization in a given sample is linearly correlated with its diffraction efficiency, the conclusion of this analysis can be turned to account to measure the global initiation efficiency of any radical toward any monomer. By way of illustration, the original approach introduced here is applied to the study of the dye-sensitized polymerization of acrylamide systems. This kinetic study of diffraction growth curve is based on the fact that in this kind of material a modulation of the refractive index goes together with the monomer conversion.

Since the rate of the polymerization—here, under weak conditions of irradiation—depends on the square root of the absorbed dose of incident light, the simplest model introduced by Kogelnik, on which most of the studies of photochemical systems are based, is rather difficult to handle. The results reported in this paper exemplify a new approach to this question and show how, when combined with time-resolved laser spectroscopy experiments, the hologram growth curves can be interpreted.

Obviously, this approach could be improved. In particular, and provided that this type of study is extended to other MB/amine systems, a careful analysis of the $\phi$ would allow the part played by the purely electronic effects relative to the steric effects to be pointed out in the study of the reactivity of a set of amine-derived radicals toward a given monomer.

In conclusion, the interest of the use of the techniques based on holography is to allow direct and nondestructive measurements in living polymer films in which kinetic information is often difficult to extract. One of the big drawbacks of these techniques is that they give only very little information about specific details of chemical reactions. However, the exemplification reported here shows

that when coupled with other time-resolved techniques, holographic spectroscopy becomes a very powerful tool for photochemical studies.

Moreover, the theoretical approach developed in this paper might be very useful for the study of many recent applications of holography that are being developed for their practical interest, e.g., optical memories or commutation systems, and that are in need of fundamental research.[38]

## Appendix

$\Lambda$: fringe spacing

$$\Lambda = \lambda/(2 \sin \theta)$$

$I$: intensity of each writing beam.
$I_R$: intensity of the reading beam.
$I_D$: intensity of the diffracted beam at the instant $t$.
$\eta$: diffraction efficiency

$$\eta = I_D/I_R$$

$I_T$: intensity of each transmitted writing beam at $t$.
$I_{abs}$: intensity absorbed by the sample for each writing beam at $t$

$$I_{abs} = I - I_T$$

OD: macroscopic optical density under holographic exposure at $t$

$$OD = \log I/I_T$$

At the point $x$ and the instant $t$ under holographic exposure: $OD(x,t)$ = optical density

$$OD = (1/\Lambda) \int_0^\Lambda OD(x,t) \, dx$$

$I(x)$: incident intensity

$$I(x) = 2I(1 + \cos 2\pi x/\Lambda) \qquad (1)$$

$I_{abs}(x,t)$: absorbed intensity

$$I_{abs}(x,t) = 2I(1 + \cos 2\pi x/\Lambda)(1 - 10^{-OD(x,t)}) \qquad (3)$$

$I_T(x,t)$: transmitted intensity

$$I_T(x,t) = I(x) - I_{abs}(x,t)$$

$$I_T = (1/2\Lambda) \int_0^\Lambda I_T(x,t) \, dx$$

[$\bar{M}$]: average concentration of the monomer in the sample (since the conversion never exceeds 15% in the experiments reported here, the monomer concentration at the point $x$ and the time $t$ [M($x,t$)] can be replaced by its average value [$\bar{M}$].
$R_p$: rate of photopolymerization.
$\rho(x,t)$: local percent of double bonds having disappeared at time $t$.
$\bar{\rho}(t)$: average percent of double bonds polymerized at time $t$

$$\bar{\rho}(t) = (1/\Lambda) \int_0^\Lambda \rho(x,t) \, dx$$

$n$: refractive index

$$n(x,t) = n_0 + NA(x,t)(1 + \cos 2\pi x/\Lambda)^{1/2} \qquad (5)$$

$N$: constant depending on the polymerizable system.
$n_0$: refractive index at the instant $t = 0$.

$n_1(t)$: refractive index modulation.

Under homogeneous conditions of irradiation (with only one red beam).

$T$: IR transmission of the sample after irradiation.

$T_0$: IR transmission of the sample before irradiation.

$\rho$: percent of double bonds having disappeared after irradiation

$$\rho = 100 \frac{\log T - \log T_0}{\log T_0} = \frac{100}{[\bar{M}]} \int_0^t R_p \, dt$$

$$A(x,t) = \int_{t_0}^{t} (1 - 10^{-OD(x,t)})^{1/2} \, dt$$

$$B_r(t) = \int_{OD_{t=0}}^{OD_t} \frac{d(OD)}{(1 - 10^{-OD})^r}$$

$$B_1(t) = B(t)$$

$\phi$: overall initiation yield of the photopolymerization.
$\phi_{MB}$: overall MB photolysis yield.
$\phi_{ST}$: intersystem crossing quantum yield.

**Registry No.** DMAA, 2680-03-7; AA, 79-06-1; MBAA, 110-26-9; MB, 61-73-4; TEA, 102-71-6; DEA, 111-42-2; EA, 141-43-5; BEA, 67362-76-9; DMBA, 103-83-3.

## References and Notes

(1) Tomlinson, W. J.; Chandross, E. A. *Adv. Photochem.* **1980**, *12*, 201.
(2) Feinberg, J. *SPIE* **1985**, *532*, 119.
(3) Bräuchle, C.; Burland, D. M. *Angew. Chem., Int. Ed. Engl.* **1983**, *22*, 582, and references cited therein. Deeg, F. W.; Pinsl, J.; Bräuchle, C. *J. Phys. Chem.* **1986**, *90*, 5710. Pinsl, J.; Deeg, F. W.; Bräuchle, C. *Appl. Phys. B* **1986**, *40*, 77. Deeg, F. W.; Pinsl, J.; Bräuchle, C. *IEEE J. Quantum Electron.* **1986**, *QE-22*, 1476. Pinsl, J.; Gehrtz, M.; Bräuchle, C. *J. Phys. Chem.* **1986**, *90*, 6754.
(4) Burland, D. M. *Acc. Chem. Res.* **1983**, *16*, 218. Burland, D. M. *IEEE J. Quantum Electron.* **1986**, *QE-22*, 1469.
(5) Testa, A. C.; Wild, U. P. *J. Phys. Chem.* **1986**, *90*, 4302.
(6) Milles, D. G.; Lamb, P. D.; Rhee, K. W.; Johnson, C. S. *J. Phys. Chem.* **1983**, *87*, 4815.
(7) Marotz, J. *Appl. Phys. B* **1985**, *37*, 181.
(8) Colburn, W. S.; Haines, K. A. *Appl. Opt.* **1971**, *10*, 1636.
(9) Tomlinson, W. J.; Chandross, E. A.; Weber, H. P.; Aumiller, G. D. *Appl. Opt.* **1976**, *15*, 534.
(10) Smith, H. M. *Holographic Recording Materials*; Springer Verlag: Berlin, 1977. Solymar, L.; Cooke, D. J. *Volume Holography and Volume Gratings*; Academic: London, 1981.
(11) Su, S. F.; Gaylord, T. K. *J. Opt. Soc. Am.* **1975**, *65*, 59. Magnusson, R.; Gaylord, T. K. *J. Appl. Phys.* **1976**, *47*, 190. Magnusson, R.; Gaylord, T. K. *J. Opt. Soc. Am.* **1977**, *67*, 1165.
(12) Kogelnik, H. *Bell. Syst. Tech. J.* **1969**, *48*, 2909. Collier, R. J.; Burckardt, C. B.; Lin, L. H. *Optical Holography*; Academic: New York, 1971.
(13) Champetier, G.; Buvet, R.; Neel, J.; Sigwalt, P. *Chimie Macromoléculaire*; Hermann: Paris, 1970; p 82.
(14) Sugawara, S.; Murase, K.; Kitayama, T. *Appl. Opt.* **1975**, *14*, 378. Sugawara, S. *Rev. Electr. Commun. Lab.* **1976**, *24*, 301.
(15) Chesneau, E.; Fouassier, J. P. *Angew. Makromol. Chem.* **1985**, *135*, 41.
(16) Lorimer, J. W. *Polymer* **1972**, *13*, 46. Lorimer, J. W. *Polymer* **1972**, *13*, 274.
(17) Shibata, J. H.; Johnson, C. S. *Appl. Spectrosc.* **1985**, *39*, 786.
(18) Tomlinson, W. J. *Appl. Opt.* **1976**, *15*, 821.
(19) Urbach, J. C.; Meier, R. W. *Appl. Opt.* **1969**, *8*, 2269.
(20) Richter, K. H.; Güttler, W.; Schwoerer, M. *Appl. Phys. A* **1983**, *32*, 1.
(21) Marotz, J. *Appl. Phys. B* **1985**, *37*, 181.
(22) Todorov, T.; Markovski, P.; Tomova, N.; Dragostinova, V.; Stoyanova, K. *Opt. Quantum Electron.* **1984**, *16*, 471.
(23) Calvert, J. G.; Pitts, J. N. *Photochemistry*; Wiley: New York, 1966.
(24) Lougnot, D. J., Thèse 3ème Cycle, Mulhouse, 1972. Carré, C.; Lougnot, D. J. *J. Chim. Phys.* **1988**, *85*, 485.
(25) Kamat, P. V.; Lichtin, N. N. *J. Phys. Chem.* **1981**, *85*, 3864.
(26) Pileni, M. P.; Grätzel, M. *J. Phys. Chem.* **1980**, *84*, 2402.
(27) Kubota, T.; Ose, T.; Sasaki, M.; Honda, K. *Appl. Opt.* **1976**, *15*, 556.
(28) Kayser, R. H.; Young, R. H. *Photochem. Photobiol.* **1976**, *24*, 395. Kayser, R. H.; Young, R. H. *Photochem. Photobiol.* **1976**, *24*, 403.
(29) Léger, L.; Hervet, H.; Rondelez, F. *Macromolecules* **1981**, *14*, 1732. Antonietti, M.; Coutandin, J.; Grütter, R.; Sillescu, H. *Macromolecules* **1984**, *17*, 798.
(30) Smith, B. A. *NATO ASI Ser., Ser C* **1986**, *182*, 397.
(31) Zhang, J.; Wang, C. H.; Chen, Z. X. *J. Chem. Phys.* **1986**, *85*, 5359.
(32) Wopschall, R. H.; Pampalone, T. R. *Appl. Opt.* **1972**, *11*, 2096.
(33) Bonneau, R. Thèse d'Etat, Bordeaux, 1971. Solar, S.; Getoff, N.; Solar, W.; Mark, F. *Radiat. Phys. Chem.* **1981**, *17*, 107.
(34) Nilsson, R.; Merkel, P. B.; Kearns, D. R. *Photochem. Photobiol.* **1972**, *16*, 109. Ohno, T.; Osif, T. L.; Lichtin, N. N. *Photochem. Photobiol.* **1976**, *30*, 541.
(35) Fouassier, J. P. *J. Chim. Phys.* **1983**, *80*, 339.
(36) Koroleev, B. A.; Mal'tseva, M. A.; Tarasou, A. I.; Vasnev, U. A. *J. Gen. Chem. USSR* **1974**, *44*, 864.
(37) Aue, D. H.; Webb, H. M.; Bowers, M. T. *J. Am. Chem. Soc.* **1976**, *98*, 311.
(38) Carré, C.; Ritzenthaler, D.; Lougnot, D. J.; Fouassier, J. P. *Opt. Lett.* **1987**, *12*, 646. Lougnot, D. J.; Ritzenthaler, D.; Carré, C.; Fouassier, J. P. *J. Appl. Phys.* **1988**, *63*, 4841.